ACS OMEGA

http://pubs.acs.org/journal/acsodf

Article

C−C Bond Formation Reaction Catalyzed by a Lithium Atom: Benzene-to-Biphenyl Coupling

Hiroto Tachikawa*

Cite This: *ACS Omega* 2023, 8, 10600−10606

Read Online

ACCESS | Metrics & More | Article Recommendations | Supporting Information

ABSTRACT: Transition-metal-catalyzed carbon−carbon (C−C) bond formation is an important reaction in pharmaceutical and organic chemistry. However, the reaction process is composed of multiple steps and is expensive owing to the presence of transition metals. This study proposes a lithium-catalyzed C−C coupling reaction of two benzene molecules (Bz) to form a biphenyl molecule, which is a transition-metal-free reaction, based on ab initio and direct ab initio molecular dynamics (AIMD) calculations. The static ab initio calculations indicate that the reaction of two Bz molecules with Li^- ions (reactant state, RC) can form a stable sandwiched complex (precomplex), where the Li^- ion is sandwiched by two Bz molecules. The complex formation reaction can be expressed as $2Bz + Li^- \rightarrow Bz(Li^-)Bz$, where the C−C distance between the Bz rings is 2.449 Å. This complex moves to the transition state (TS) via the structural deformation of $Bz(Li^-)Bz$, where the C−C distance is shortened to 2.118 Å. The barrier height was calculated to be −9.9 kcal/mol (relative to RC) at the MP2/6-311++G(d,p) level. After TS, the $C(sp^3)$-$C(sp^3)$ single bond was completely formed between the Bz rings (the C−C bond distance was 1.635 Å) (late complex). After the dissociation of H_2 from the late complex, a biphenyl molecule was formed: the $C(sp^2)$−$C(sp^2)$ bond. The calculations suggest that the C−C bond coupling of Bz occurred spontaneously from $2Bz + Li^-$, and biphenyl molecules were directly formed without an activation barrier. Direct AIMD calculations show that the C−C coupling reaction also takes place under electron attachment to $Li(Bz)_2$: $Li(Bz)_2 + e^- \rightarrow [Li^-(Bz)_2]_{ver} \rightarrow$ precomplex $\rightarrow$ TS $\rightarrow$ late complex, where $[Li^-(Bz)_2]_{ver}$ is the vertical electron capture species of $Li(Bz)_2$. Namely, the C−C coupling reaction spontaneously occurred in $Li(Bz)_2$ owing to electron attachment. Similar C−C coupling reactions were also observed for halogen-substituted benzene molecules (Bz−X, X = F and Cl). Furthermore, this study discusses the mechanism of C−C bond formation in electron capture based on the theoretical results.

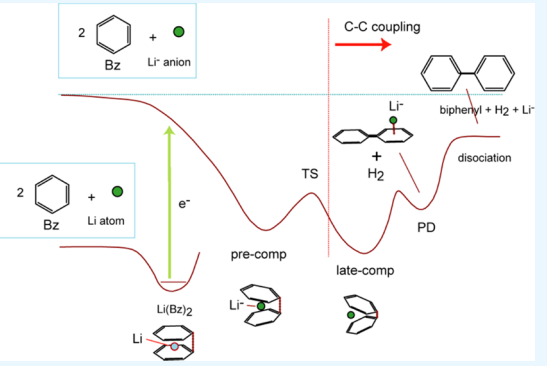

1. INTRODUCTION

The formation of carbon−carbon $C(sp^3)$−$C(sp^3)$ bonds between molecules is important in the synthesis of molecules for various applications, such as pharmaceuticals, agrochemicals, and materials.[1−5] Cross couplings are reactions that combine different carbon substituents via the cleavage of C−C and carbon−heteroatom bonds. Tamao and Kumada et al.[6] and Corriu et al.[7] independently reported the cross-coupling reactions of alkenyl halides or aryl halides with Grignard reagents in the presence of Ni(II) catalyst.[8] Subsequently, the Suzuki−Miyaura coupling reaction, a cross-coupling reaction in the presence of a Pd catalyst using organo-halides and organo-boron compounds, was proposed.[9−13] Additionally, Negishi coupling[14−16] and Mizoroki−Heck reaction[17−19] were also proposed.

According to the proposed mechanisms of these cross-coupling reactions,[20−23] the reaction is initiated by the oxidative insertion of palladium(0) into a carbon−halogen bond of the aryl halide used as the substrate and the formation of a palladium(II) intermediate. This key step is followed by the coupling of reactants, reductive elimination of the newly formed coupled product, and regeneration of the palladium(0) center. For these cross-coupling reactions, ligands with soft donor sites are often required to stabilize the palladium(0) state and satisfy the vacant coordination sites of the palladium(II) intermediate. Bulky arylphosphines are particularly popular soft ligands for these reactions. Thus, multiple steps with transition metals are needed to achieve C−C bond formation.

Catalytic C−H activation reaction is also a powerful method for cleaving inactive C−H bonds and generating new bonds.[24,25] The process of converting to leaving groups such as halogens is not necessary, and byproducts tend to be small. However, the reaction conditions are severe and require special alignment groups to achieve chemo-selectivity.

Received: January 25, 2023
Accepted: February 24, 2023
Published: March 6, 2023

https://doi.org/10.1021/acsomega.3c00520
ACS Omega 2023, 8, 10600−10606

The present study proposes that a benzene−benzene C−C single bond is formed spontaneously via the catalytic reaction of lithium anion (Li^-). A schematic illustration of the concept used in the present study is shown in Figure 1.

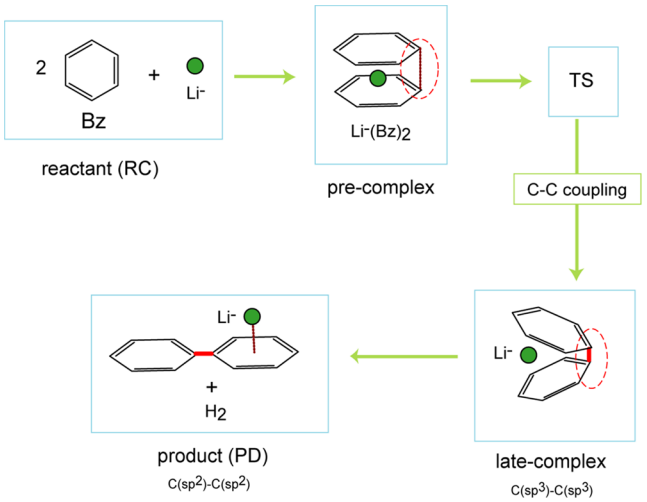

Figure 1. Reaction scheme of the present study. Bz, Li^-, and TS mean benzene molecule, lithium anion, and transition state, respectively.

The initial state was composed of two benzene molecules (Bz) and an Li^- anion (reactant state, RC). Mixing of these species forms a sandwich-type complex (precomplex). Structural deformation of the complex yields a C−C coupling product (late complex) via a transition state (TS). This reaction occurs at a significantly low activation barrier relative to the precomplex (2.7 kcal/mol at the MP2/6-311++G(d,p) level) and zero barrier vs RC. Namely, the Li^- anion catalyzes the C−C coupling reaction of two Bz molecules. After the dissociation of H_2 from the complex, a biphenyl molecule was formed as a product. The reaction energy was −4.3 kcal/mol, indicating that the C−C coupling reaction proceeded without activation energy. A similar reaction occurred efficiently from the neutral complex of $Li(Bz)_2$ triggered by electron attachment. The lithium used was a single atom, and no transition-metal catalyst was required. In this work, similar calculations were performed for halogen-substituted benzene molecules (Bz−X, where X = F and Cl).

In our previous report, we preliminarily demonstrated the electron capture reaction for $Li(Bz)_2$.[26] The C−C bond formation was observed. However, a detailed analysis of the full collision ($2Bz + Li^-$) was not carried out, and the zero-point vibration energy (ZPE) was not considered in the dynamics calculations. As a result, the discussion of the previous study was limited to a qualitative nature. In this study, static calculations were performed at the MP2 level, and the ZPE was included in the reaction dynamics.

2. COMPUTATIONAL DETAILS

2.1. Ab initio Calculations. Static ab initio calculations were carried out using the 6-311++G(d,p) and 6-311++G(2d,p) basis sets.[27,28] The geometries and energies were obtained using the MP2, MP4(SDQ), and CAM-B3LYP methods.[29−31] The atomic charge was calculated using the natural population analysis (NPA) method.[32,33] Standard Gaussian 09 and 16 program packages were used for all static ab initio calculations.[34,35]

2.2. Direct AIMD Calculations. Two methods were used in the direct AIMD calculations: (a) the optimized structure of $Li(Bz)_2$ as the starting structure and (b) $Li(Bz)_2$ including the zero-point vibrational energy (ZPE). In the direct AIMD calculation of $[Li(Bz)_2]^-$, $Li(Bz)_2$, was first optimized at the CAM-B3LYP/6-311G(d,p) level. Thereafter, the trajectory of $[Li(Bz)_2]^-$ was started from the vertical electron capture point. The rotational temperature, momentum vector, and excess energy of $[Li(Bz)_2]_{ver}^-$ were set to be zero (time = 0 fs), where "ver" means vertical electron capture of $Li(Bz)_2$. The maximum simulation time was 1.0 ps. The time step was 0.02 fs. The

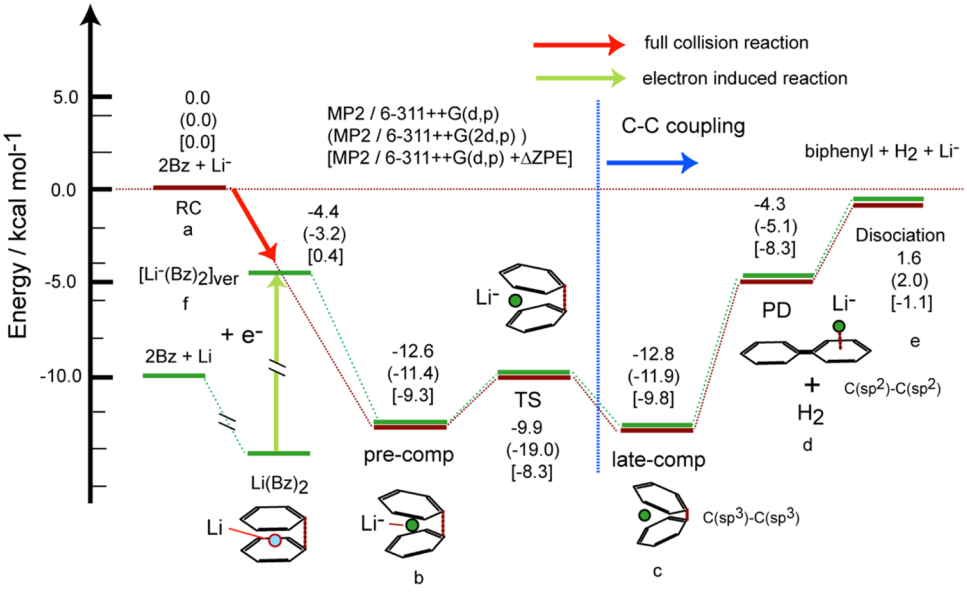

Figure 2. Schematic energy diagram for the Li^-catalyzed C−C coupling reaction from benzene to biphenyl. The relative energies are in kilocalorie per mole. The energy levels were calculated at the MP2/6-311++G(d,p) and MP2/6-311++G(2d,p) levels. ZPE means zero-point energy correction. Values without parentheses are calculated with MP2/6-311++G(d,p). Values in parentheses are from MP2/6-311++G(2d,p). Values in brackets are those calculated with MP2/6-311++G(d,p) including zero-point correction.

https://doi.org/10.1021/acsomega.3c00520
ACS Omega 2023, 8, 10600−10606

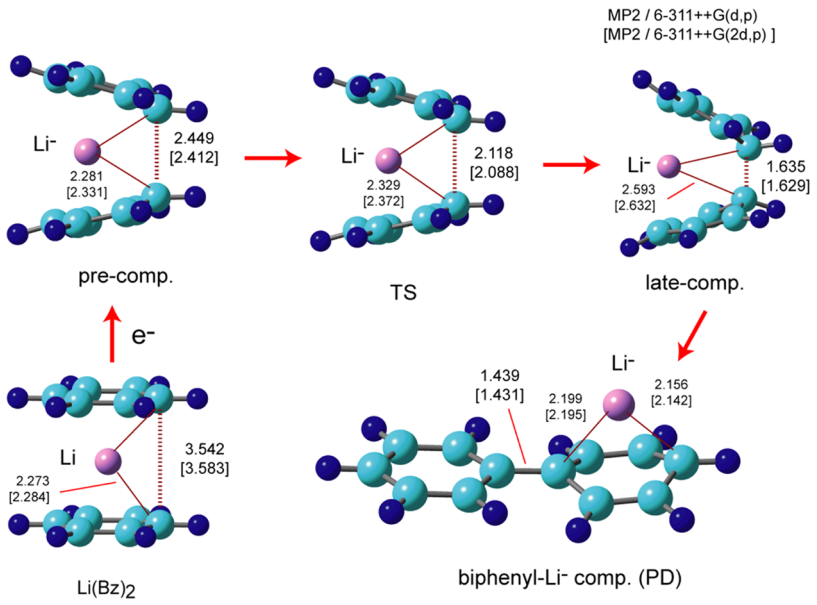

Figure 3. Optimized structures of $Li(Bz)_2$ reaction system calculated at the MP2/6-311++G(d,p) and MP2/6-311++G(2d,p) levels. Bond distances are in Å.

velocity Verlet algorithm was used to solve the equations of motion of the system. The drift in the total energy was <0.01 kcal/mol. No symmetry restriction was applied to calculate the energy gradient.

The effects of ZPE on the reaction mechanism were investigated using the classical vibrational sampling method (microcanonical ensemble).[36−38] The calculations including ZPE were performed at the CAM-B3LYP/6-31G(d) level. Direct AIMD calculations were carried out using our own code.[39−41] The drifts of the total energies were $<1.0 \times 10^{-2}$ kcal/mol in all trajectory calculations.

3. RESULTS

3.1. Energy Diagram for the C−C Coupling Reaction.

Figures 2 and 3 show the energy diagram of the C−C coupling reaction of two benzene molecules (Bz) to form a biphenyl molecule (Biph) catalyzed by the lithium anion (Li^-) and the optimized structure at the stationary points, respectively.

The results obtained from the MP2/6-311++G(d,p) calculations are mainly discussed here. The energy diagram comprises two reaction pathways: a full collision reaction (red arrow) and an electron-induced reaction (green arrow). In the full collision reaction, three molecules, two Bz molecules and Li^- ($2Bz + Li^-$), are related to the reaction (reactant state, RC). In electron-induced reactions, the complex composed of two Bz and Li atoms, $Li(Bz)_2$, causes the reaction after electron capture. In both pathways, the C−C coupling reaction occurred after the reactions.

The reactant state (RC) in the full collision reaction was composed of two Bz molecules and Li^- ($2Bz + Li^-$, point a), where the energy level was set to zero. The Li^- anion has a positive electron affinity (0.62 eV), which is more stable than the Li atom. After the collision of Bzs with Li^-, a sandwich-type complex was formed (point b, denoted by the precomplex), where Li^- was sandwiched between two Bzs. The nearest C−C distance between the Bzs (R) was 2.449 Å, as shown in Figure 3 (precomplex), and the energy of the precomplex was −12.6 kcal/mol more stable than that of RC.

The precomplex led to a transition state (TS) with a structural change. The C−C distance decreased from R = 2.449 Å (precomplex) to 2.118 Å (TS). The energy levels of TS were calculated to be −9.9 kcal/mol (relative to RC) and +2.7 kcal/mol (relative to precomplex). After TS, the reaction point reached the late complex (point c). The C−C distance was further shortened to R = 1.635 Å (late complex), suggesting that a single C−C bond was formed from the reaction of Bz with Li^-; the C−C coupling occurred in the late complex. The energy levels of the late complex were −12.8 kcal/mol (relative to RC) and −0.2 kcal/mol (relative to precomplex). This reaction occurs as an exothermic reaction from the RC.

In the product state (PD, point d), the H_2 molecule dissociated from the late complex, and the product was biphenyl−Li^- + H_2. The C−C bond length was R = 1.439 Å. The energy level of PD was −4.3 kcal/mol (relative to RC), indicating that biphenyl molecules were formed without an activation barrier from two Bz's due to the catalyzation of Li^-. The dissociation state (biphenyl + H_2 + Li^-, point e) was slightly higher in energy than the RC (1.6 kcal/mol). However, the inclusion of ZPE decreased to −1.1 kcal/mol. A full collision reaction occurred as an almost isothermal reaction. These results strongly indicate that the C−C coupling reaction of two Bz molecules is catalyzed by Li^-.

In the electron-induced C−C coupling pathway, the initial state was the sandwiched complex $Li^-(Bz)_2$, as shown in Figure 3. The complex was formed via the reaction of two Bz molecules with a Li atom. The C−C bond distance was 3.542 Å in $Li(Bz)_2$. The reaction was initiated by the electron capture of $Li(Bz)_2$, and then $[Li^-(Bz)_2]_{ver}$ was tentatively formed (point f). The vertical electron capture point was −4.4 kcal/mol lower than that of the RC and 15.0 kcal/mol higher than that of the neutral complex $Li(Bz)_2$. The reaction point moved spontaneously to the precomplex region, where the relative energy from the RC changed to −12.6 kcal/mol. The relative energy of the TS was −9.9 kcal/mol (vs RC) and 2.7 kcal/mol higher than that of the precomplex. After the TS, the reaction point moved to the late complex, which was −12.8 kcal/mol lower in energy than that of the RC. The product state was composed of biphenyl molecule-

https://doi.org/10.1021/acsomega.3c00520
ACS Omega 2023, 8, 10600−10606

Li^- and H_2 molecule, which was −4.3 kcal/mol lower in energy than that of the RC. The energy diagram calculated at the MP2/6-311++G(2d,p) level showed similar energetics for both reaction paths.

3.2. C−C Bond Population along the Reaction. To elucidate the C−C bond formation in detail, the bond populations between C−C atoms in the bonding site (P_{CC}) were calculated for the RC, $[Li^-(Bz)_2]_{ver}$, pre- and late-complexes, TS, biphenyl−Li^- complex, and biphenyl molecules. The results are presented in Table 1.

Table 1. C−C Bond Populations In Binding Sites for $Li^-(Bz)_2$ System

state	MP2/6-311++G(d,p)	MP2/6-311++G(2d,p)
RC	0.00	0.00
VER	0.009	0.005
precomplex	0.187	0.191
TS	0.344	0.359
late complex	0.732	0.731
biphenyl-Li(−)	1.006	1.020
biphenyl	0.879	0.888

The C−C bond population was zero in the RC (P_{CC} = 0.0). The values of the C−C bond populations increased gradually as the reaction progressed: the precomplex, TS, and late complex were P_{CC} = 0.187, 0.344, and 0.732, respectively. The biphenyl−Li^- complex, the product of the reaction, has a P_{CC} value of 1.006, suggesting that the C−C single bond was formed in the late complex. Similar values were obtained at the MP2/ 6-311++G(d,p) and MP2/6-311++G(2d,p) levels.

3.3. Intrinsic Reaction Coordinate (IRC) for the C−C Coupling Reaction. As shown in the previous sections, a TS structure was found between the pre- and late-complexes. To verify the true TS, the IRC was calculated from the TS. The results are shown in Figure 4.

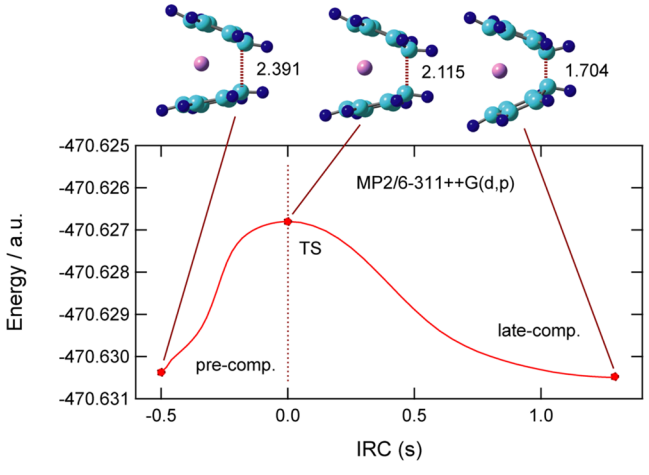

Figure 4. IRC between pre- and late-complex regions calculated at the MP2/ 6-311++G(d,p) level.

The potential energy curve of the IRC shows that the TS is connected smoothly to both the pre- and late-complex regions. The C−C bond in the binding site gradually shortened as the reaction proceeded. This result strongly suggests that the TS is the true saddle point in the C−C coupling reaction in $Li^-(Bz)_2$.

Similar calculations were performed at the CAM-B3LYP/6-311++G(d,p) level. The results are shown in Figure S1 in the Supporting Information (SI). The calculation shows that the TS was located between the pre- and late-complexes in the C−C coupling reaction.

3.4. Reaction Dynamics of C−C Coupling Reaction. Direct AIMD calculations were performed for the electron-induced reaction path to determine the time scale of the reaction. First, the structure of $Li(Bz)_2$ was fully optimized at the CAM-B3LYP/6-311G(d,p) level. Next, the reaction of $(Li(Bz)_2)^-$ after vertical electron capture of the neutral complex, $Li(Bz)_2$, was tracked via direct AIMD calculations. The time propagation of the potential energy of the system $(Li^-(Bz)_2)$ following electron capture is shown in Figure 5.

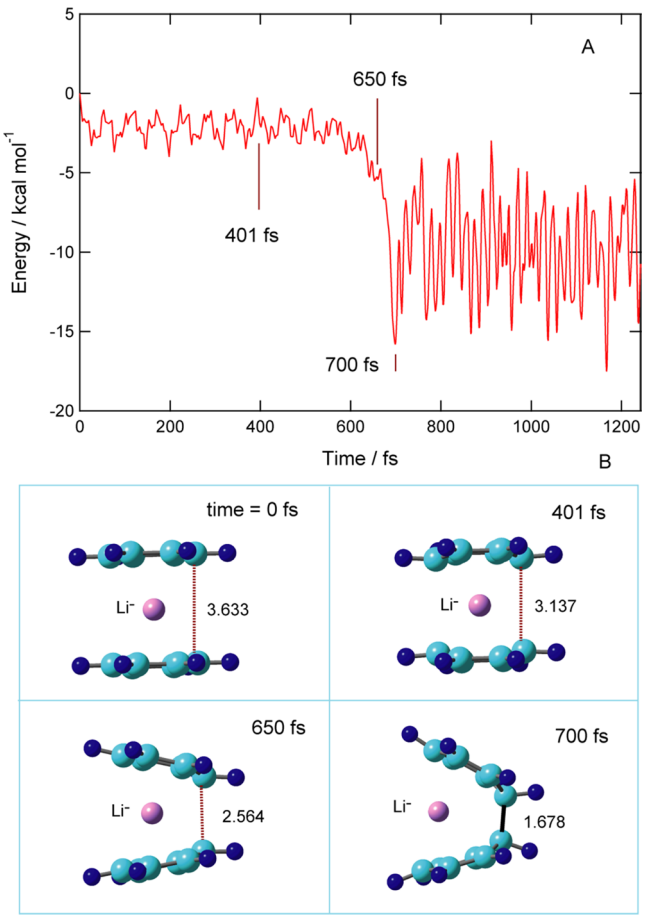

Figure 5. (A) Time evolution of potential energy of $Li^-(Bz)_2$ after vertical electron capture of the neutral complex $Li(Bz)_2$, and (B) snapshots of $Li^-(Bz)_2$. Bond distances are in Å. The calculation was carried out at the CAM-B3LYP/6-311G(d,p) level starting from the optimized structure.

After the electron capture of $Li(Bz)_2$, the energy decreased rapidly to −3.0 kcal/mol at 10 fs due to the rapid structural deformation of the benzene rings. Subsequently, this energy periodically vibrated. Both Bz rings were gradually closer to each other: R = 3.137 Å at 401 fs, which is 0.496 Å shorter than that at time zero. At 650 fs, the intermolecular distance was R = 2.564 Å, and the energy was −5.0 kcal/mol. At 650−700 fs, the potential energy suddenly decreased to −15.0 kcal/mol. This drastic change was caused by the formation of a single C−C bond between the two benzene rings: R = 1.678 Å at 700 fs. These

https://doi.org/10.1021/acsomega.3c00520
ACS Omega 2023, 8, 10600−10606

results indicate that the C−C single bond was directly formed after the electron capture of $Li(Bz)_2$.

Similar direct AIMD calculations were carried out using the M062X and wB97X functionals on the 6-311++G(d,p) basis. The results are shown in Figures S1 and S3. Both calculations show that the C−C coupling reactions occurred in $Li(Bz)_2$ after the electron capture.

3.5. Effects of Zero-point Energy (ZPE) on the Reaction Mechanism. Direct AIMD calculations, including ZPE calculations, were performed at the CAM-B3LYP/6-31G(d) level. Twenty trajectories were performed, six of which are shown in Figure S4. The reaction time for the C−C bond formation was distributed in the range of 205.3−426.8 fs, with an average of 300.0 fs. In contrast, the reaction time in the absence of ZPE was 449.6 fs. These results indicate that the ZPE accelerated the reaction time for C−C bond formation.

3.6. Effects of Halogen Substitution (X = F and Cl). In this section, the effects of halogen substitution on the reaction mechanism are discussed. All of the calculations were performed at the CAM-B3LYP/6-311G(d,p) level of theory. First, one of the hydrogen atoms of the benzene molecule in $Li(Bz)_2$ was substituted with an F atom, and the geometry of (F−Bz)Li(Bz) was subsequently optimized. Direct AIMD calculations were performed for $(F-Bz)Li(Bz)^-$ from the vertical electron capture point. The results are shown in Figure 6.

After the electron capture of (F−Bz)Li(Bz), the energy decreased rapidly to −3.0 kcal/mol at 10 fs due to the rapid structural deformation of the benzene rings. Subsequently, the energy gradually decreased. At approximately 400 fs, the energy suddenly decreased and reached a minimum at 423 fs. The distances of F−Bz from Bz drastically changed to R = 3.488 Å (time = 0 fs), 2.704 Å (310 fs), and 1.660 Å (423 fs), indicating that the carbon atom of F−Bz gradually approached and collided with the carbon atom of Bz at 423 fs. After the collision, a new C−C bond was formed between F−Bz and Bz at 513 fs (R = 1.637 Å). The new C−C bond was located in ortho-position relative to the F-atom. A similar C−C coupling reaction was observed for X = Cl, as shown in Figure S5.

To check the position of C−C coupling, direct AIMD calculations were carried out from several initial configurations of F-Bz relative to Li^-Bz. The calculations showed that the C−C coupling products are found in the meta- and ortho-positions. In contrast, there was no para-position product. These results suggest that there is regioselectivity in this C−C coupling reaction.

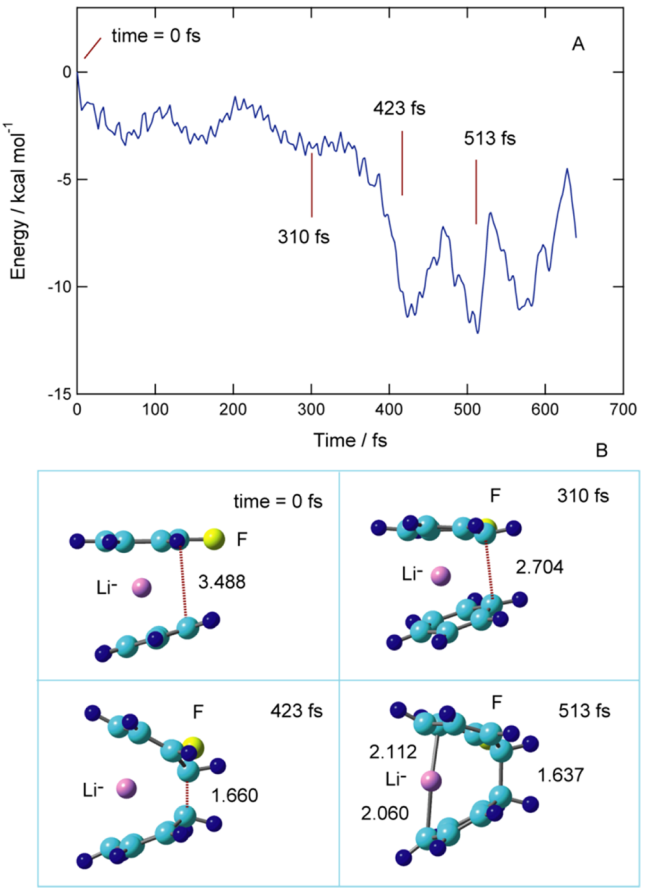

Figure 6. Effects of halogen substitution on the reaction mechanism. (A) Time evolution of potential energy of Li^-(F-Bz)(Bz) after vertical ionization of the neutral complex Li(F-Bz)(Bz), and (B) snapshots of Li^-(F-Bz)(Bz). Bond distances are in Å. The calculation was carried out at the CAM-B3LYP/6-311G(d,p) level starting from the optimized structure.

4. DISCUSSION AND CONCLUSIONS

As a summary of the present study, a schematic illustration of the reaction mechanism is given in Figure 7. The reaction state (RC) was composed of two benzene molecules (Bz) and an Li^- anion. The reaction of these species produced a precomplex, where the Li^- anion was sandwiched between two Bz molecules. After the transition state (TS), a late complex was formed, where the C−C bond was shortened to 1.635 Å, suggesting that the C−C coupling was completed in the late complex (the C−C bond population was P_{CC} = 0.733). Next, the biphenyl−Li^- complex was formed via the dissociation of H_2, where P_{CC} = 1.066 and the C−C bond length was 1.440 Å (the normal bond length of the C−C bond). In the final state, a biphenyl molecule was formed as a product. These results indicate that the C−C coupling reaction occurs spontaneously from two Bz molecules and an Li^- anion.

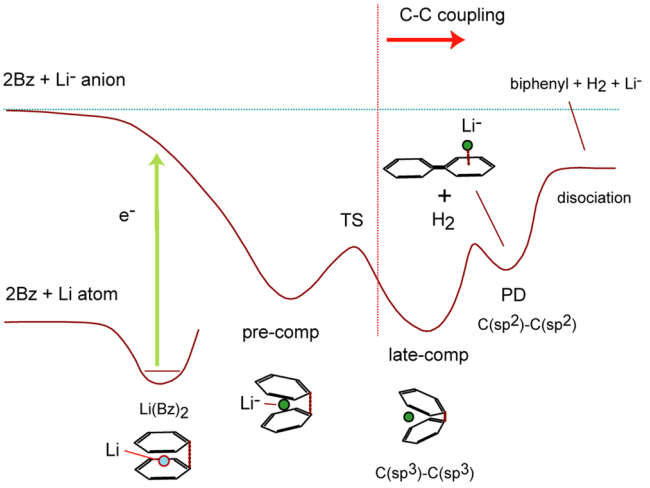

Figure 7. Schematic energy diagram for the Li-catalyzed C−C coupling reaction from benzene to biphenyl obtained on the basis of the present study.

Overall, this study demonstrates another reaction route as the C−C coupling reaction to form biphenyl. The lower curve indicates the formation of a sandwiched neutral complex, $Li(Bz)_2$, via the reaction of two Bz molecules with an Li atom. After the electron capture of $Li(Bz)_2$, a precomplex was formed

https://doi.org/10.1021/acsomega.3c00520
ACS Omega 2023, 8, 10600−10606

as an intermediate, and the reaction produced the biphenyl molecule. The time scale of the C−C coupling reaction was less than 1.0 ps, indicating that the C−C coupling catalyzed by Li^- occurs as a fast process after electron capture.

■ ASSOCIATED CONTENT

Supporting Information

The Supporting Information is available free of charge at https://pubs.acs.org/doi/10.1021/acsomega.3c00520.

SI is available on the ACS website: IRC calculated at the CAM-B3LYP/ 6-311++G(d,p) level, results of direct AIMD calculations at the M062X/6-311G(d,p) and wB97XD/6-311G(d,p) levels, the effects of ZPE on reaction time and mechanism, and the effects of Cl substitution on the reaction mechanism are provided in the SI (PDF)

■ AUTHOR INFORMATION

Corresponding Author

Hiroto Tachikawa − *Division of Applied Chemistry, Faculty of Engineering, Hokkaido University, Kita-ku, Sapporo 060-8628, Japan;* orcid.org/0000-0002-7883-2865; Email: hiroto@eng.hokudai.ac.jp

Complete contact information is available at: https://pubs.acs.org/10.1021/acsomega.3c00520

Notes

The author declares no competing financial interest.

■ ACKNOWLEDGMENTS

The authors acknowledge partial support from JSPS KAKENHI (Grant Numbers: 21H05415 and 21K04973).

■ REFERENCES

(1) Biffis, A.; Centomo, P.; Del Zotto, A.; Zecca, M. Pd Metal Catalysts for Cross-couplings and Related Reactions in the 21st Century: A Critical Review. *Chem. Rev.* **2018**, *118*, 2249−2295.

(2) Magano, J.; Dunetz, J. R. Large-scale Applications of Transition Metal-catalyzed Couplings for the Synthesis of Pharmaceuticals. *Chem. Rev.* **2011**, *111*, 2177−2250.

(3) Everson, D. A.; Weix, D. J. Cross-electrophile Coupling: Principles of Reactivity and Selectivity. *J. Org. Chem.* **2014**, *79*, 4793−4798.

(4) Gu, J.; Wang, X.; Xue, W.; Gong, H. Nickel-catalyzed Reductive Coupling of Alkyl Halides with Other Electrophiles: Concept and Mechanistic Considerations. *Org. Chem. Front.* **2015**, *2*, 1411−1421.

(5) Choi, J.; Fu, G. C. Transition Metal-catalyzed Alkyl-alkyl Bond Formation: Another Dimension in Cross-coupling Chemistry. *Science* **2017**, *356*, No. eaaf7230.

(6) Tamao, K.; Sumitani, K.; Kumada, M. J. Selective Carbon-carbon Bond Formation by Cross-coupling of Grignard Reagents with Organic Halides. Catalysis by Nickel-phosphine Complexes. *J. Am. Chem. Soc.* **1972**, *94*, 4374.

(7) Corriu, R. J. P.; Massse, J. P. Activation of Grignard Reagents by Transition-metal Complexes. A New and Simple Synthesis of Trans-stilbenes and Polyphenyls. *J. Chem. Soc., Chem. Commun.* **1972**, 144a.

(8) Fujii, I.; Semba, K.; Nakao, Y. The Kumada-Tamao-Corriu Coupling Reaction Catalyzed by Rhodium-aluminum Bimetallic Complexes. *Org. Lett.* **2022**, *24*, 3075−3079.

(9) Miyaura, N.; Yanagi, T.; Suzuki, A. The Palladium-catalyzed Cross-coupling Reaction of Phenylboronic Acid with Haloarenes in the Presence of Bases. *Synth. Commun.* **1981**, *11*, 513−519.

(10) Miyaura, N.; Yamada, K.; Suzuki, A. A New Stereospecific Cross-coupling by the Palladium-catalyzed Reaction of 1-Alkenylboranes with 1-Alkenyl or 1-alkynyl Halides. *Tetrahedron Lett.* **1979**, *20*, 3437−3440.

(11) Yamamoto, Y.; Takada, S.; Miyaura, N.; Iyama, T.; Tachikawa, H. γ-Selective Cross-coupling Reactions of Potassium Allyltrifluoroborates with Haloarenes Catalyzed by a Pd(0)/D-t-BPF or Pd(0)/Josiphos ((R,S)-CyPF-t-Bu) Complex: Mechanistic Studies on Transmetalation and Enantioselection. *Organometallics* **2009**, *28*, 152−160.

(12) Ishiyama, T.; Miyaura, N.; Suzuki, A. Syntheses of Functionalized Organotin Compounds via Palladium-catalyzed Cross-coupling Reaction of Aryl or 1-Alkenyl Halides with 9-(ω-Stannylalkyl)-9-borabicyclo[3.3.1]nonanes. *Synlett* **1991**, 687−688.

(13) Hooshmand, S. E.; Heidari, B.; Sedghi, R.; Varma, R. S. Recent Advances in the Suzuki-Miyaura Cross-coupling Reaction Using Efficient Catalysts in Eco-friendly Media. *Green Chem.* **2019**, *21*, 381−405.

(14) Negishi, E.-i. Magical Power of Transition Metals: Past, Present, and Future (Nobel Lecture). *Angew. Chem., Int. Ed.* **2011**, *50*, 6738−6764.

(15) Negishi, E.-I.; King, A. O.; Okukado, N. Selective Carbon-carbon Bond Formation via Transition Metal Catalysis. 3. A Highly Selective Synthesis of Unsymmetrical Biaryls and Diarylmethanes by the Nickel- or Palladium-catalyzed Reaction of Aryl- and Benzylzinc Derivatives with Aryl Halide. *J. Org. Chem.* **1977**, *42*, 1821−1823.

(16) Haas, D.; Hammann, J. M.; Greiner, R.; Knochel, P. Recent Developments in Negishi Cross-coupling Reactions. *ACS Catal.* **2016**, *6*, 1540−1552.

(17) Heck, R. F.; Nolley, J. P. Palladium-catalyzed Vinylic Hydrogen Substitution Reactions with Aryl, Benzyl, and Styryl Halides. *J. Org. Chem.* **1972**, *37*, 2320−2322.

(18) Heck, R. F. The Palladium-catalyzed Arylation of Enol Esters, Ethers, and Halides. A New Synthesis of 2-Aryl Aldehydes and Ketones. *J. Am. Chem. Soc.* **1968**, *90*, 5535−5538.

(19) Mizoroki, T.; Mori, K.; Ozaki, A. Arylation of Olefin with Aryl Iodide Catalyzed by Palladium. *Bull. Chem. Soc. Jpn.* **1971**, *44*, 581.

(20) Hansmann, M. M.; Pernpointner, M.; Doepp, R.; Hashmi, A. S. K. A Theoretical DFT-based and Experimental Study of the Transmetalation Step in Au/Pd-mediated Cross-coupling Reactions. *Chem. - Eur. J.* **2013**, *19*, 15290−15303.

(21) Zhang, T. −X.; Li, Z. A DFT Study on Pd-catalyzed Suzuki Cross-coupling Polycondensation of Aryl Bromide Monomers. *Comput. Theor. Chem.* **2013**, *1016*, 28−35.

(22) Gourlaouen, C.; Ujaque, G.; Lledos, A.; Medio-Simon, M.; Asensio, G.; Maseras, F. Why Is the Suzuki-Miyaura Cross-coupling of sp^3 Carbons in α-Bromo Sulfoxide Systems Fast and Stereoselective? A DFT Study on the Mechanism. *J. Org. Chem.* **2009**, *74*, 4049−4054.

(23) Düfert, M. A.; Billingsley, K. L.; Buchwald, S. L. Suzuki-Miyaura Cross-Coupling of Unprotected, Nitrogen-Rich Heterocycles: Substrate Scope and Mechanistic Investigation. *J. Am. Chem. Soc.* **2013**, *135*, 12877−12885.

(24) Hartwig, J. F. Evolution of C−H Bond Functionalization from Methane to Methodology. *J. Am. Chem. Soc.* **2016**, *138*, 2−24.

(25) Davies, H. M. L.; Morton, D. Recent Advances in C−H Functionalization. *J. Org. Chem.* **2016**, *81*, 343−350.

(26) Tachikawa, H. Alkali Metal Mediated C-C Bond Coupling Reaction. *J. Chem. Phys.* **2015**, *142*, No. 064301.

(27) McLean, A. D.; Chandler, G. S. Contracted Gaussian-Basis Sets for Molecular Calculations. I. Second Row Atoms, Z=11-18. *J. Chem. Phys.* **1980**, *72*, 5639−5648.

(28) Head-Gordon, M.; Head-Gordon, T. Analytic MP2 Frequencies Without Fifth Order Storage: Theory and Application to Bifurcated Hydrogen Bonds in the Water Hexamer. *Chem. Phys. Lett.* **1994**, *220*, 122−128.

(29) Head-Gordon, M.; Pople, J. A.; Frisch, M. J. MP2 Energy Evaluation by Direct Methods. *Chem. Phys. Lett.* **1988**, *153*, 503−506.

(30) Krishnan, R.; Frisch, M. J.; Pople, J. A. Contribution of Triple Substitutions to the Electron Correlation Energy in Fourth-Order Perturbation Theory. *Chem. Phys. Lett.* **1980**, *72*, 4244−4245.

(31) Yanai, T.; Tew, D.; Handy, N. A New Hybrid Exchange-correlation Functional Using the Coulomb-attenuating Method (CAM-B3LYP). *Chem. Phys. Lett.* **2004**, *393*, 51−57.

(32) Reed, A. E.; Curtiss, L. A.; Weinhold, F. Intermolecular Interactions from a Natural Bond Orbital, Donor-Acceptor Viewpoint. *Chem. Rev.* **1988**, *88*, 899−926.
(33) Reed, A. E.; Weinhold, F. Natural Atomic Orbitals and Natural Population Analysis. *J. Chem. Phys.* **1983**, *78*, 4066−4073.
(34) Frisch, M. J.; Trucks, G. W.; Schlegel, H. B.; Scuseria, G. E.; Robb, M. A.; Cheeseman, J. R.; Scalmani, G.; Barone, V.; Mennucci, B.; Petersson, G. A.; et al., *Gaussian 09*, revision D.01; Gaussian, Inc.: Wallingford, CT, 2013.
(35) Frisch, M. J.; Trucks, G. W.; Schlegel, H. B.; Scuseria, G. E.; Robb, M. A.; Cheeseman, J. R.; Scalmani, G.; Barone, V.; Petersson, G. A.; et al., *Gaussian 16*, Revision A.03; Gaussian, Inc.: Wallingford, CT, 2016.
(36) Schlegel, H. B.; Millam, J. M.; Iyengar, S. S.; Voth, G. A.; Daniels, A. D.; Scuseria, G. E.; Frisch, M. J. Ab initio Molecular Aerodynamics: Propagating the Density Matrix with Gaussian Orbitals. *J. Chem. Phys.* **2001**, *114*, 9758−9763.
(37) Iyengar, S. S.; Schlegel, H. B.; Millam, J. M.; Voth, G. A.; Scuseria, G. E.; Frisch, M. J. Ab initio Molecular Dynamics: Propagating the Density Matrix with Gaussian Orbitals. II. Generalizations based on Mass-weighting, Idempotency, Energy Conservation and Choice of Initial Conditions. *J. Chem. Phys.* **2001**, *115*, 10291−10302.
(38) Schlegel, H. B.; Iyengar, S. S.; Li, X.; Millam, J. M.; Voth, G. A.; Scuseria, G. E.; Frisch, M. J. Ab initio molecular dynamics: Propagating the Density Matrix with Gaussian Orbitals. III. Comparison with Born-Oppenheimer Dynamics. *J. Chem. Phys.* **2002**, *117*, 8694−8704.
(39) Tachikawa, H. Reaction Mechanism of an Intracluster S_N2 Reaction Induced by Electron Capture. *Phys. Chem. Chem. Phys.* **2022**, *24*, 3941−3950.
(40) Tachikawa, H. Reaction Dynamics of NO^+ with Water Clusters. *J. Phys. Chem. A* **2022**, *126*, 119−124.
(41) Tachikawa, H. Reactions of Photoionization-Induced CO-H_2O Cluster: Direct Ab Initio Molecular Dynamics Study. *ACS Omega* **2021**, *6*, 16688−16695.

https://doi.org/10.1021/acsomega.3c00520
ACS Omega 2023, 8, 10600−10606